Stratigraphic coordinates, a coordinate system tailored to seismic interpretation[a]

[a]Published in Geophysical Prospecting, v. 63, 1246-1255, (2015)

Parvaneh Karimi and Sergey Fomel

ABSTRACT

In certain seismic data processing and interpretation tasks, such as spiking deconvolution, tuning analysis, impedance inversion, spectral decomposition, etc., it is commonly assumed that the vertical direction is normal to reflectors. This assumption is false in the case of dipping layers and may therefore lead to inaccurate results. To overcome this limitation, we propose a coordinate system in which geometry follows the shape of each reflector and the vertical direction corresponds to normal reflectivity. We call this coordinate system *stratigraphic coordinates*. We develop a constructive algorithm that transfers seismic images into the stratigraphic coordinate system. The algorithm consists of two steps. First, local slopes of seismic events are estimated by plane-wave destruction; then structural information is spread along the estimated local slopes, and horizons are picked everywhere in the seismic volume by the predictive-painting algorithm. These picked horizons represent level sets of the first axis of the stratigraphic coordinate system. Next, an upwind finite-difference scheme is used to find the two other axes, which are perpendicular to the first axis, by solving the appropriate gradient equations. After seismic data are transformed into stratigraphic coordinates, seismic horizons should appear flat, and seismic traces should represent the direction normal to the reflectors. Immediate applications of the stratigraphic coordinate system are in seismic image flattening and spectral decomposition. Synthetic and real data examples demonstrate the effectiveness of stratigraphic coordinates.

INTRODUCTION

In certain seismic data processing and interpretation tasks, such as spiking deconvolution, tuning analysis, impedance inversion, spectral decomposition, etc., it is commonly assumed that the vertical direction is normal to reflectors. This assumption does not hold true in the case of dipping layers and may therefore lead to inaccurate results (Guo and Marfurt, 2010). Mallet (2004) defined a mathematical framework, called GeoChron, for transforming the geologic space into a new space in which all horizons appear flat, and faults, if any, disappear. In this paper, we propose the

stratigraphic coordinate system, in which geometry follows the shape of each reflector and the vertical direction corresponds to normal reflectivity .

Flattening post-stack seismic data is an immediate use of the proposed coordinate system. Flattened seismic images facilitate the interpreter's ability to extract detailed stratigraphic information from the seismic data. In interpretational applications, several different algorithms for image flattening have been developed by different authors. The idea of seismic image flattening by extracting stratal slices was introduced by Zeng et al. (1998). Automatic picking of horizons using local shifts was studied by Bienati and Spagnolini (1999) and Stark (2005). Lomask et al. (2006) and Parks (2010) presented inversion methods in which horizons are calculated on the basis of local slopes and are then used to flatten seismic events. Fomel (2010) proposed the method of predictive painting that uses the prediction operators extracted by plane-wave destruction to spread information inside the seismic volume recursively.

Conventionally, seismic image flattening is performed by shifting samples in the original image up or down - in other words, differentially stretching and squeezing the original image in order to flatten the reflection events. Luo and Hale (2013) proposed a method for image flattening that uses the vector shift field instead of the scalar field of vertical shifts to define deformations in the image. Flattening by vector shift uses either vertical shear or rotation or a combination of the two, depending on the type of geologic deformation.

The stratigraphic coordinate system, introduced in this paper, represents a new framework for seismic interpretation and processing. To construct stratigraphic coordinates, we combine predictive painting with an upwind finite-difference scheme (Franklin and Harris, 2001) for solving relevant gradient equations. The stratigraphic coordinate system is semi-orthogonal; i.e., picked horizons that are level sets of the first axis are orthogonal to the other two axes. In other words, stratigraphic coordinates are aligned with horizons, and the vertical direction in stratigraphic coordinates corresponds to the direction normal to the major reflection boundaries. Application of the stratigraphic coordinate system is not limited to seismic image flattening and may be extended to many data processing and interpretation tasks in which the vertical direction is commonly assumed to be normal to reflection boundaries: a crude assumption in all structures but flat geology. In the following sections, we start by describing a constructive algorithm for generating stratigraphic coordinates. We then illustrate applications of the stratigraphic coordinate system to seismic image flattening and spectral decomposition using synthetic and field data examples.

THEORY

In order to define the first step for transformation to stratigraphic coordinates, we follow the predictive-painting algorithm (Fomel, 2010), which is reviewed in appendix A. Predictive painting spreads the time values along a reference trace into the seismic volume to output the *relative geologic age* attribute ($Z_0(x, y, z)$). The painted

horizons output by predictive painting are used as the first axis of our stratigraphic coordinate system. Several alternative methods exist to track horizons automatically in a seismic volume and produce horizon cubes (Hoyes and Cheret, 2011; Wolak et al., 2013). We choose predictive painting because of its simplicity and efficiency.

In the next step, we find the two other axes, $X_0(x,y,z)$ and $Y_0(x,y,z)$, orthogonal to the first axis, $Z_0(x,y,z)$, by numerically solving the following gradient equations:

$$\nabla Z_0 \cdot \nabla X_0 = 0 \tag{1}$$

and

$$\nabla Z_0 \cdot \nabla Y_0 = 0. \tag{2}$$

Equations 1 and 2 simply state that the X_0 and Y_0 axes should be perpendicular to Z_0. We can define the boundary condition for the first gradient equation (equation 1) as

$$X_0(x,y,0) = x \tag{3}$$

and the boundary condition for equation 2 as

$$Y_0(x,y,0) = y. \tag{4}$$

These two boundary conditions mean that the stratigraphic coordinate system and the regular coordinate system (x,y,z) become equivalent at the surface $(z=0)$.

The stratigraphic coordinates are originally designed for depth images. When applied to time-domain images, the definition of the gradient operator becomes

$$\nabla = \left(\frac{\partial}{\partial x}, \frac{\partial}{\partial y}, \frac{\partial}{\partial z}\frac{\partial z}{\partial t}\right), \tag{5}$$

so a scaling factor with dimensions of velocity-squared is needed in equations 1 and 2.

Algorithm

In summary, our algorithm for transferring seismic images from the regular Cartesian coordinate system into the stratigraphic coordinate system consists of the following steps:

1. Extract the first axis of the stratigraphic coordinate system $Z_0(x,y,z)$ from seismic image $P(x,y,z)$ by predictive painting;

2. Start with X_0 at $(z=0)$ as an initial value and solve equation 1 with boundary condition 3 numerically for X_0;

3. Start with Y_0 at $(z=0)$ as an initial value and solve equation 2 with boundary condition 4 numerically for Y_0.

We solve equations 1 and 2 numerically with an explicit upwind finite-difference scheme (Franklin and Harris, 2001; Li and Fomel, 2013).

EXAMPLES OF STRATIGRAPHIC COORDINATES

For a simple illustration of stratigraphic coordinates, we use a 2D synthetic seismic image from Claerbout (2006), which contains layers with sinusoidal dip variations, faulted and truncated by an unconformity, and dipping beds with constant slope above the unconformity (Figure 1a). Figure 1b shows local slopes measured by plane-wave destruction and delineates the slope field variation. Figure 2a shows automatically picked horizons obtained by the predictive-painting algorithm. After solving the gradient equation 1, we acquire the other axis of the stratigraphic coordinate system (Figure 2b). Figure 3a shows the stratigraphic coordinates grid overlain on the regular Cartesian coordinates of the seismic image. Complex tectonic deformations expressed in faults and folds cannot in general be undone by a simple vertical stretch and squeeze operator. In contrast, the transformation to stratigraphic coordinates allows for complex displacements, which can better capture and thus undo non-trivial tectonic deformations. Arrows in Figure 3b show the amount and direction of shift that it takes for different samples to be transformed from their original position in the seismic image to their corresponding positions in the flattened image through the stratigraphic coordinates algorithm. For comparison, arrows in Figure 3c represent how different samples shift under conventional flattening methods. The seismic image gets flattened when the data from the regular coordinate system are transferred to stratigraphic coordinates. The result is shown in Figure 4a. Apart from the structural (fault) and stratigraphic (erosional truncation) discontinuities, the input image is successfully flattened. Figure 4b shows that by returning from stratigraphic coordinates to regular coordinates, one can recostruct the features of the original image effectively.

Figure 5a shows the input image for a field-data test reproduced from Lomask et al. (2006) and Fomel (2010). The input is a depth-migrated 3-D image with structural folding and angular unconformities. The three axes of the stratigraphic coordinates are shown in Figure 6. Figure 7a displays the image in the regular Cartesian coordinates overlain by its stratigraphic coordinates grid. The flattened image in the stratigraphic coordinate system, shown in Figure 7b, can be transferred back to the regular Cartesian coordinates to reconstruct the original image (Figure 7c).

APPLICATION OF STRATIGRAPHIC COORDINATES TO SPECTRAL DECOMPOSITION

Improving the accuracy of spectral decomposition is one of the possible applications of the stratigraphic coordinate system. Spectral decomposition is a window-based analysis to characterize the reflecting wavelet of an interpretation target and refers to any method that produces a continuous time-frequency analysis of a seismic trace (Partyka and Lopez, 1999). According to the convolutional model, seismic traces are considered as normal-incidence 1D seismograms, which is true in the case of horizontal layers and allows for capturing the signal wavelet while performing spectral decompo-

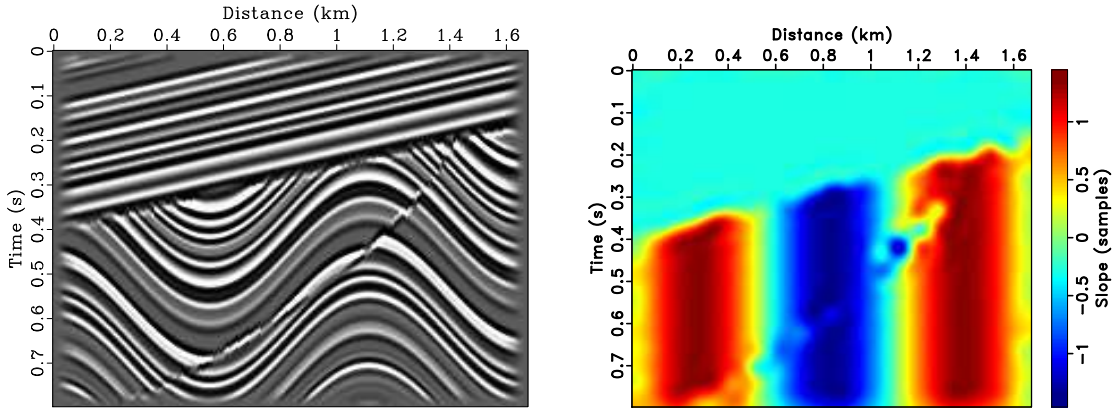

(a) (b)

Figure 1: (a) Synthetic seismic image from Claerbout (2006). (b) Local slopes measured by plane-wave destruction.

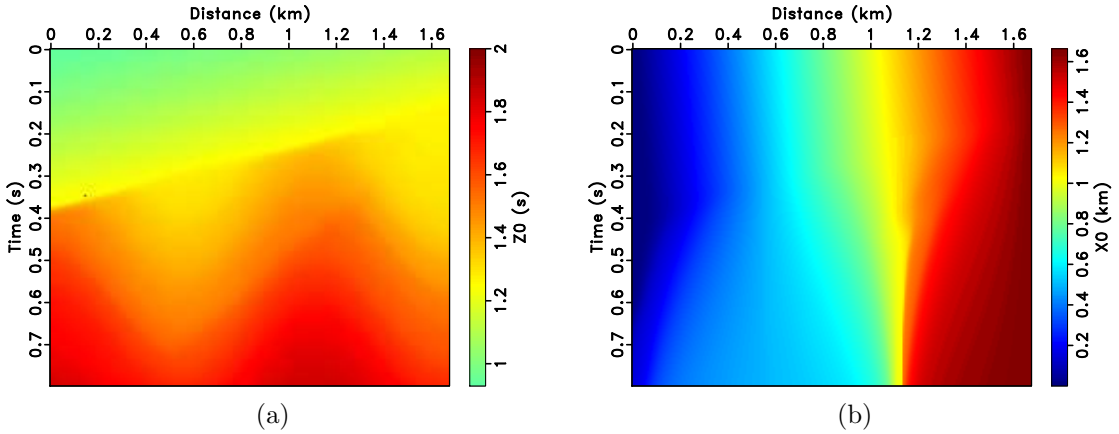

(a) (b)

Figure 2: (a) First axis (Z_0) of stratigraphic coordinates in the regular coordinates obtained by predictive painting. (b) Second axis (X_0) of the stratigraphic coordinate system acquired by solving the gradient equation (equation 1).

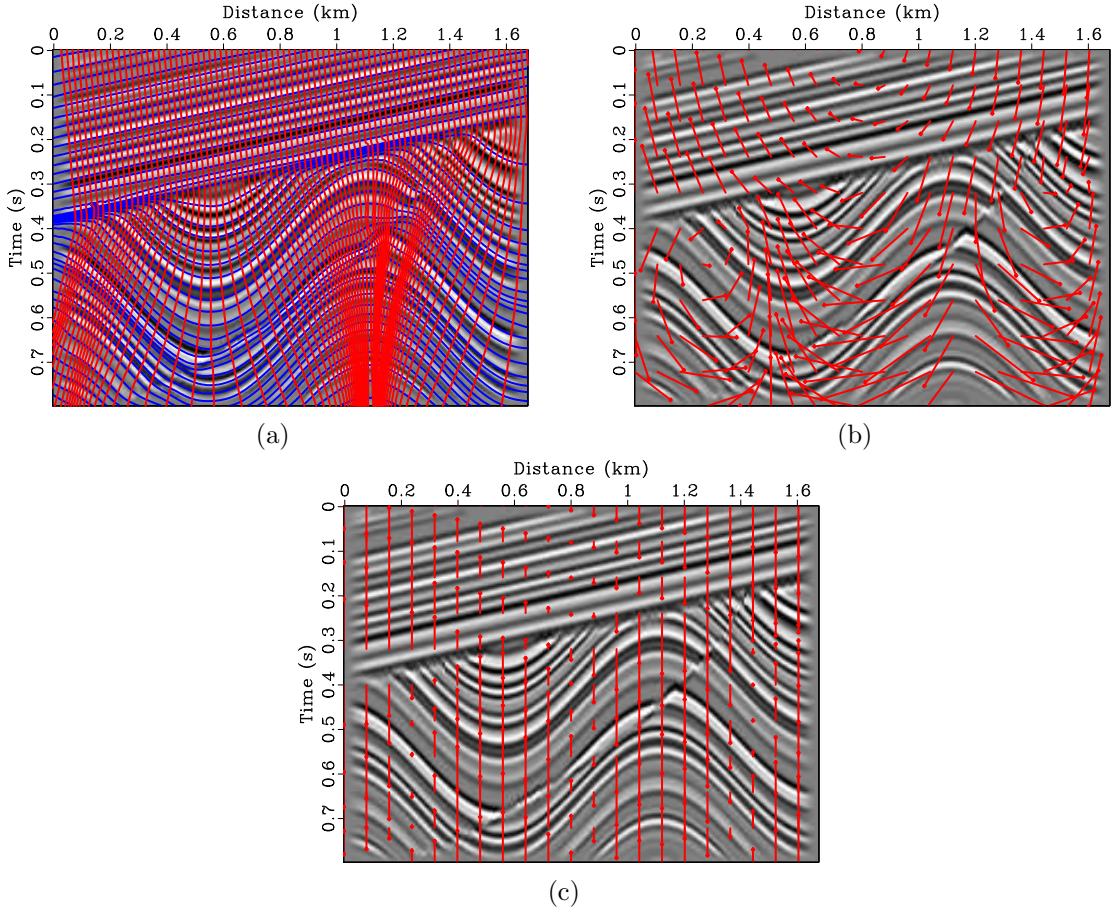

Figure 3: (a) Two axes of the stratigraphic coordinate system relative to the regular coordinate system. The synthetic image with corresponding shift represented by red arrows through using stratigraphic coordinates (b) and conventional flattening methods (c).

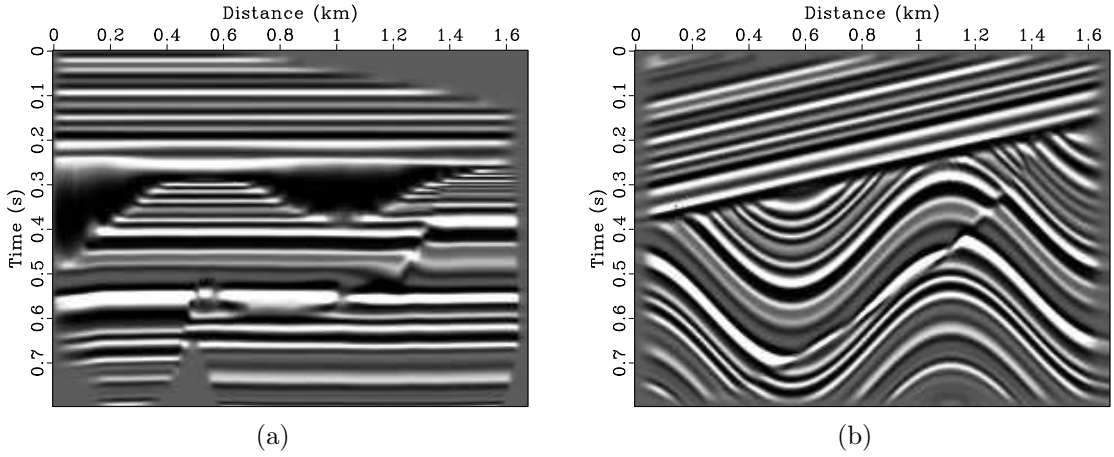

Figure 4: (a) Synthetic image from Figure 1a flattened by transferring the image to the stratigraphic coordinate system. (b) Unflattened synthetic image reconstruction by returning from stratigraphic coordinates to regular coordinates.

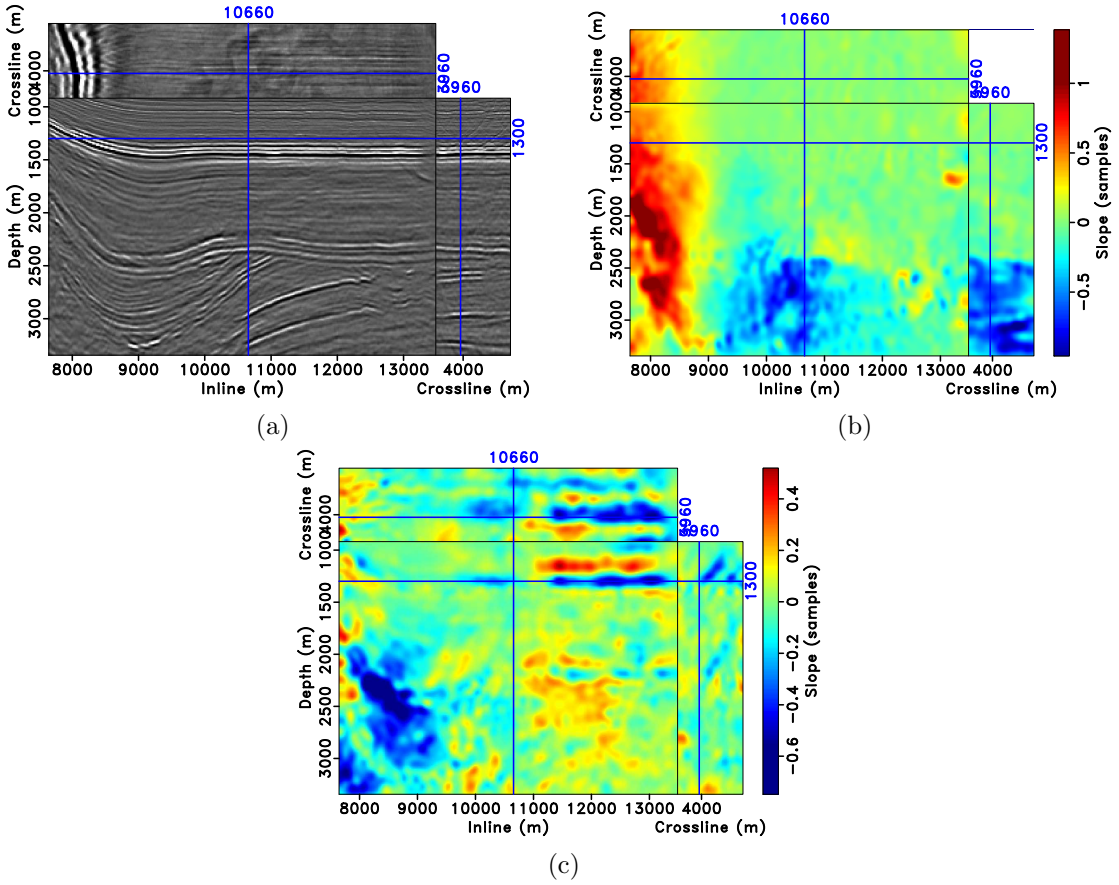

Figure 5: (a) North Sea image from Lomask et al. (2006) and its inline (b) and cross-line (c) slopes estimated by plane-wave destruction.

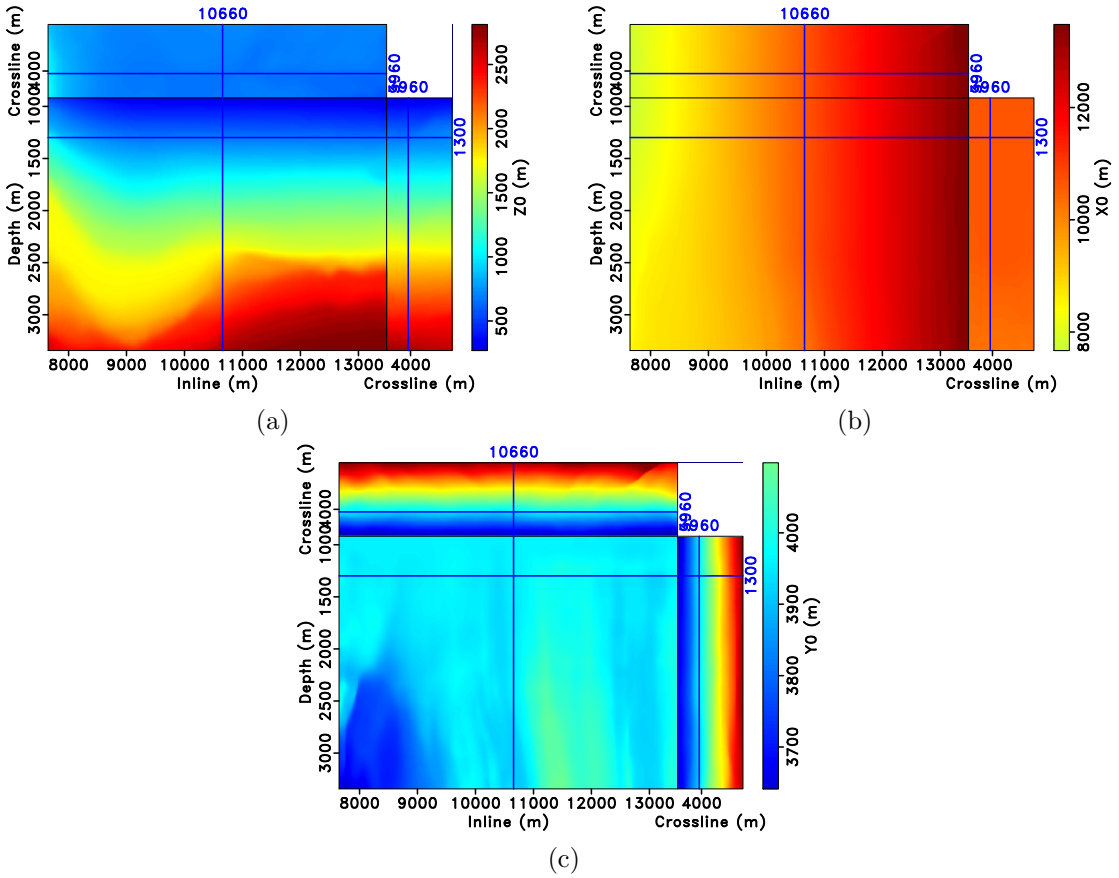

Figure 6: (a) First axis (Z_0), (b) second axis (X_0), and (c) third axis (Y_0) of stratigraphic coordinates in the North Sea image.

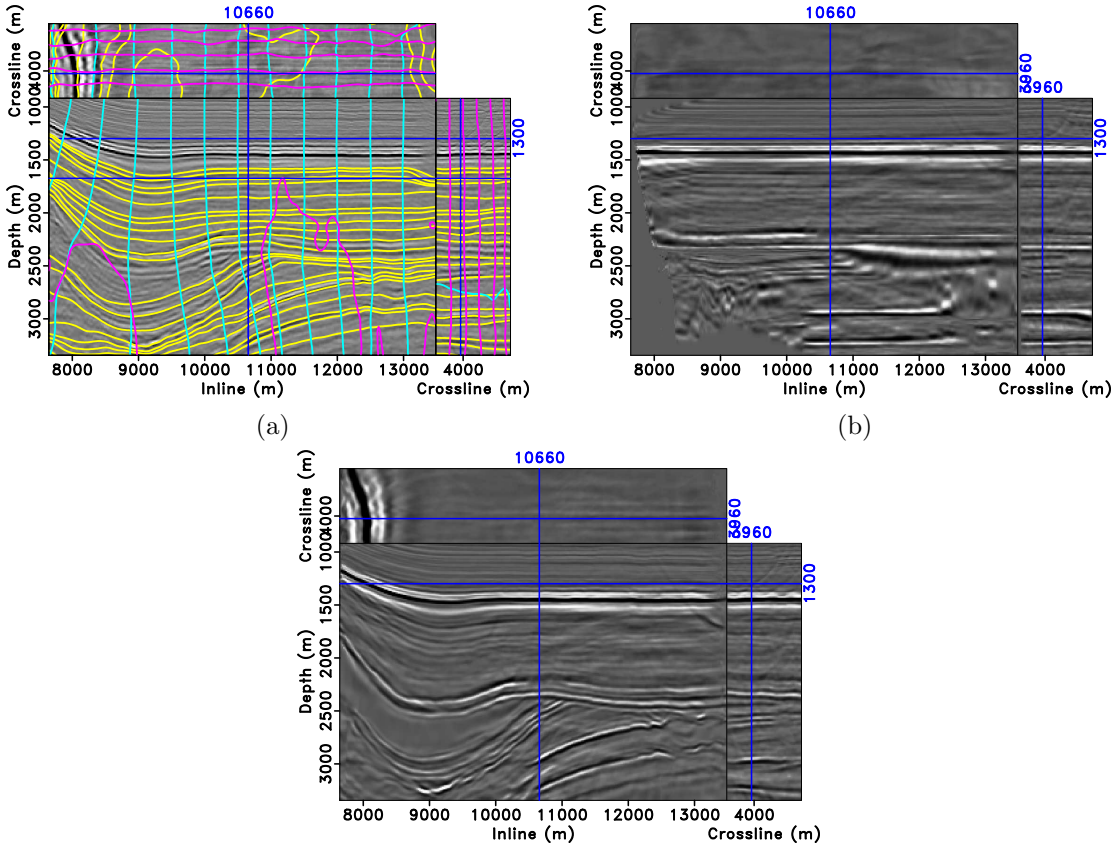

Figure 7: (a) Three axes of stratigraphic coordinates of Figure 5a plotted as a grid in their Cartesian coordinates. (b) North Sea image after flattening (transferring image to stratigraphic coordinates). (c) North Sea image reconstruction by returning from stratigraphic coordinates to regular coordinates.

sition along the seismic trace. However, when the subsurface exhibits dipping layers, the convolutional model no longer holds true, and sampling the seismic waveform vertically instead of perpendicularly to reflectors introduces a dip-dependent stretch that will carry over to any frequency estimation or spectral decomposition. Guo and Marfurt (2010) proposed to solve this problem by sampling the signal wavelet along the ray-path on which the wavelet travels. Because this path is normal to reflectors, we implement the same idea by employing the stratigraphic coordinate system, which honors the convolutional model and can capture and analyze seismic waveforms perpendicularly to seismic reflectors. Figure 8 shows Gulf of Mexico data reproduced from Lomask et al. (2006) and Liu et al. (2011) that contain a salt dome and horizons that dip steeply on the flank of the dome because of the salt piercement. Following Liu et al. (2011) we calculated the spectral decomposition of the data in the Cartesian coordinate system. Figure 9 shows horizon slices from spectral decomposition calculated in the Cartesian coordinate system at different frequencies because depositional elements of different thicknesses tune it at different frequencies. Figure 10 also shows the same horizon slices as Figure 9, but this time from spectral decomposition calculated in the stratigraphic coordinate system. Compared with horizon slices in Figure 9, those from spectral decomposition calculated in the stratigraphic coordinate system better highlight detailed geologic features such as sand channels. That is because in the stratigraphic coordinates seismic horizons get flattened and the vertical direction corresponds to the normal direction to reflectors. We can therefore analyze the unbiased seismic wavefrom and achieve a more accurate spectral decomposition result. Indeed, since seismic reflectors appear flat in the stratigraphic coordinate system, (vertical) trace analysis methods such as spectral decomposition probe the unbiased seismic waveform and thus yield more accurate measurements and attributes. Conversely, methods such as post-stack seismic inversion, spiking deconvolution, tuning analysis, etc., usually assume that layers are flat and might therefore lead interpreters to incur errors in the presence of dips. The same methods, just like spectral decomposition, may benefit from being applied in the stratigraphic coordinate system and thereby produce results unbiased by structural dip.

DISCUSSION AND CONCLUSIONS

We have introduced the stratigraphic coordinate system, a novel framework for seismic interpretation. Our algorithm for constructing the stratigraphic coordinate system consists of two steps. In the first step, we use predictive painting to produce an implicit horizon volume that defines the first axis of the stratigraphic coordinates, aligned with reflection boundaries (seismic horizons). We obtain the remaining two axes of the stratigraphic coordinate system by solving the relevant gradient equations using an upwind finite-difference scheme. Seismic image flattening is an immediate application of stratigraphic coordinates. Other possible applications include post-stack impedance inversion, tuning analysis, spiking deconvolution, or any other process that implicitly assumes that reflectors are flat or that the seismic waveforms should be sampled vertically. In all structures but layercake geology, trace-based attributes

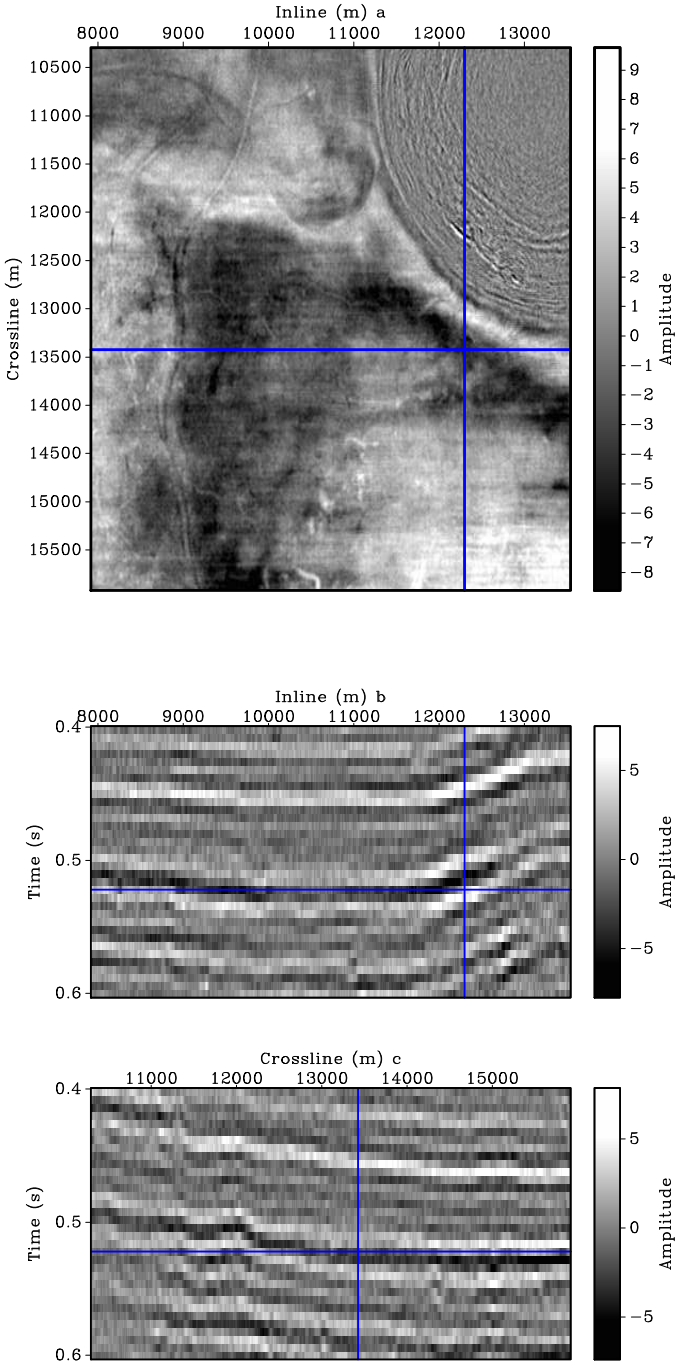

Figure 8: Seismic image from Gulf of Mexico. (a) Time slice. (b) Inline section. (c) Cross-line section.

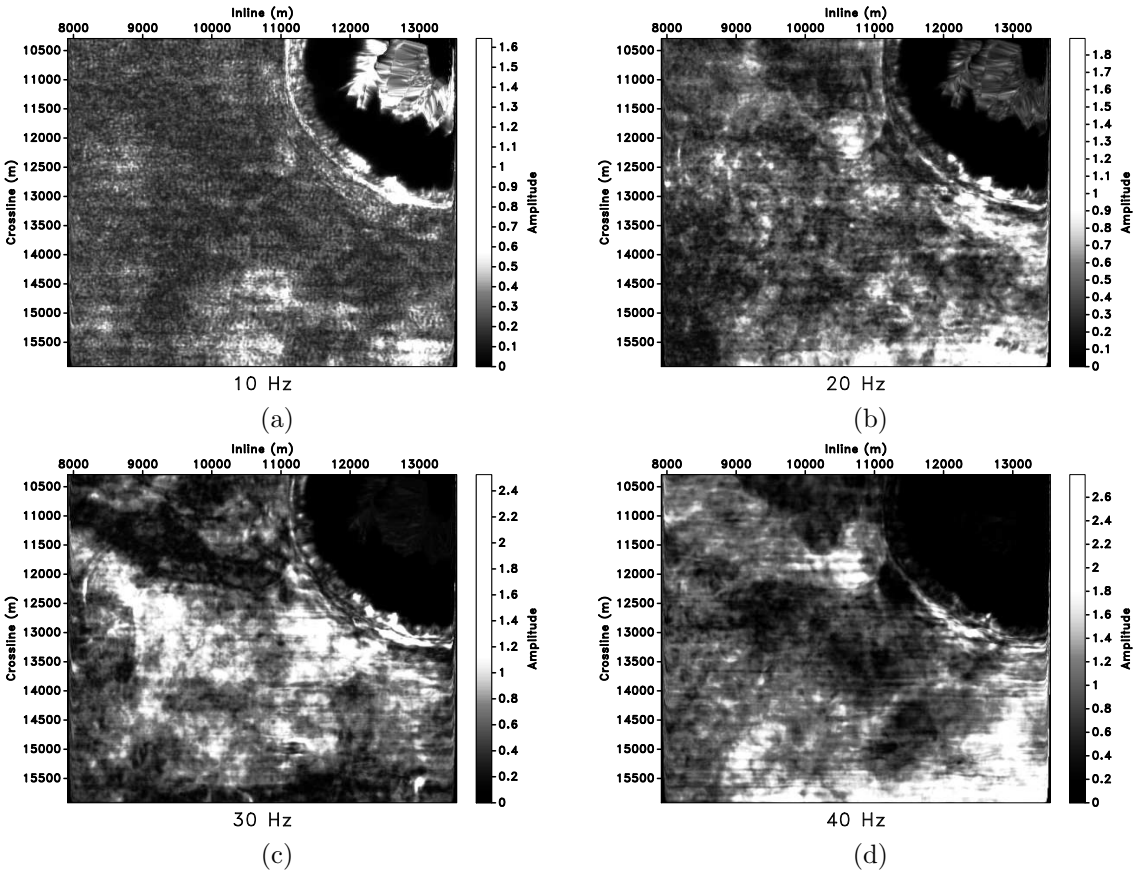

Figure 9: Horizon slices from spectral decomposition at (a) 10 Hz, (b) 20 Hz, (c) 30 Hz, and (d) 40 Hz in Cartesian coordinate system.

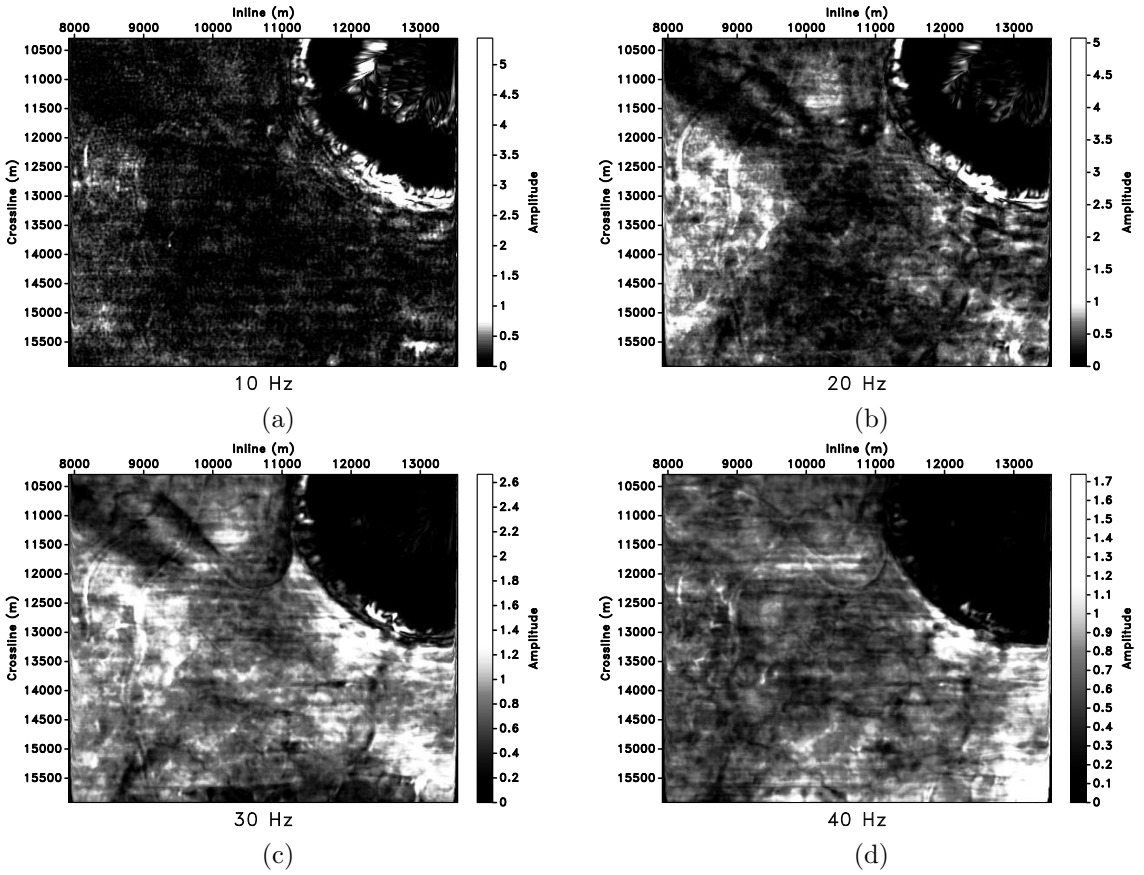

Figure 10: Horizon slices from spectral decomposition at (a) 10 Hz, (b) 20 Hz, (c) 30 Hz, and (d) 40 Hz in stratigraphic coordinate system. The 30 Hz slice most clearly displays visible channel features (red arrows).

can be biased in the presence of dipping layers. In contrast, the stratigraphic coordinate system offers a local reference frame naturally oriented to sample the unbiased seismic waveform and, hence, promises to yield more accurate waveform analysis and trace attributes.

Our implementation of stratigraphic coordinates is based on the predictive-painting algorithm, which produces the best results when traces can be predicted by their neighbors. Note that the predictive-painting algorithm may fail to capture some of the events across structural or stratigraphic discontinuities. Also, in the presence of crossing dips or incoherent events, predictive painting is susceptible to errors and warrants further improvement.

ACKNOWLEDGMENTS

We thank Stephane Gesbert and other reviewers for their valuable comments and suggestions.

APPENDIX A: PREDICTIVE PAINTING

In the most general case, the predictive-painting method (Fomel, 2010) can be described as follows:

Local spatially-variable inline and cross-line slopes of seismic events are estimated by the plane-wave destruction method (Fomel, 2002). Plane-wave destruction originates from a local plane-wave model for characterizing seismic data, which is based on the plane-wave differential equation (Claerbout, 1992):

$$\frac{\partial P}{\partial x} + \sigma \frac{\partial P}{\partial t} = 0. \tag{A-1}$$

Here $P\left(t,x\right)$ is the seismic wave-field at time t and location x, and σ is the local slope, which can be either constant or variable in both time and space. The local plane differential equation can easily be solved where the slope is constant, and it has a simple general solution

$$P\left(t,x\right) = f\left(t-\sigma x\right), \tag{A-2}$$

where $f\left(t\right)$ is an arbitrary waveform. Equation A-2 is just a mathematical description of a plane wave. In the case of variable slopes, a local operator is designed to propagate each trace to its neighbors by shifting seismic events along their local slopes.

By writing the plane-wave destruction operation in the linear operator notation, we have

$$\mathbf{r} = \mathbf{D}\mathbf{s}, \tag{A-3}$$

where $\mathbf{s}$ is a seismic section as a collection of traces $\left(\mathbf{s} = [s_1 s_2 \dots s_N]^T\right)$, $\mathbf{r}$ is the destruction residual, and $\mathbf{D}$ is the destruction operator, defined as

$$\mathbf{D} = \begin{bmatrix} \mathbf{I} & 0 & 0 & \dots & 0 \\ \mathbf{P}_{1,2} & \mathbf{I} & 0 & \dots & 0 \\ 0 & -\mathbf{P}_{2,3} & \mathbf{I} & \dots & 0 \\ \dots & \dots & \dots & \dots & \dots \\ 0 & 0 & \dots & -\mathbf{P}_{N-1,N} & \mathbf{I} \end{bmatrix}. \tag{A-4}$$

$\mathbf{I}$ is the identity operator, and $\mathbf{P}_{i,j}$ is an operator that predicts trace j from trace i. By minimizing the prediction residual $\mathbf{r}$ using least-squares optimization and smooth regularization, the dominant slopes will be obtained. For $3D$ structure characterization, a pair of inline and crossline slopes, $\sigma_x(t,x,y)$ and $\sigma_y(t,x,y)$, and a pair of destruction operators, $\mathbf{D}_x$ and $\mathbf{D}_y$, are required. The prediction of trace $\mathbf{s}_k$ from reference trace $\mathbf{s}_r$ can be defined as $\mathbf{P}_{r,k}\mathbf{s}_r$, where

$$\mathbf{P}_{r,k} = \mathbf{P}_{k-1,k} \dots \mathbf{P}_{r+1,r+2}\mathbf{P}_{r,r+1}. \tag{A-5}$$

This is a simple recursion, and $\mathbf{P}_{r,k}$ is called the predictive-painting operator. After obtaining elementary prediction operators in equation A-4 by plane-wave destruction, predictive painting spreads the information contained in a seed trace to its neighbors by following the local slope of seismic events. In order to be able to paint all events in the seismic volume, one can use multiple references and average painting values extrapolated from different reference traces.

REFERENCES

Bienati, N., and U. Spagnolini, 1999, Surface slice generation and interpretation: A review: IEEE Transactions on Geoscience and Remote Sensing, **39**, 1287–1290.

Claerbout, J. F., 1992, Earth sounding analysis: Processing versus inversion: Blackwell Science.

———, 2006, Basic earth imaging: Stanford Exploration Project.

Fomel, S., 2002, Applications of plane-wave destruction filters: Geophysics, **67**, no. 6, 1946–1960.

———, 2010, Predictive painting of 3-D seismic volumes: Geophysics, **75**, no. 4, A25–A30.

Franklin, J. B., and J. M. Harris, 2001, A fast marching level set method for monotonically advancing fronts: Computational Acoustics, **9**, 1095–1109.

Guo, H., and K. J. Marfurt, 2010, Spectral decomposition along the travel path of signal wavelets: Expanded Abstracts 80^{th} SEG International Convention, 1478–1482.

Hoyes, J., and T. Cheret, 2011, A review of "global" interpretation methods for automated 3D horizon picking: The Leading Edge, **30**, 38–47.

Li, S., and S. Fomel, 2013, Kirchhoff migration using eikonal-based computation of traveltime source-derivatives: Geophysics, **78**, no. 4, S211–S219.

Liu, G., S. Fomel, and X. Chen, 2011, Time-frequency analysis of seismic data using local attributes: Geophysics, **76**, no. 6, P23–P34.

Lomask, J., A. Guitton, S. Fomel, J. Claerbout, and A. Valenciano, 2006, Flattening without picking: Geophysics, **71**, no. 4, P12–P20.

Luo, S., and D. Hale, 2013, Unfaulting and unfolding 3d seismic images: Geophysics, **78**, no. 4, O45–O56.

Mallet, J. L., 2004, Space-time mathematical framework for sedimentary geology: Mathematical Geology, **36**, A25–A30.

Parks, D., 2010, Seismic image flattening as a linear inversion problem: Master thesis, Colorado School of Mines.

Partyka, G. A., and J. Lopez, 1999, Interpretational applications of spectral decomposition in reservoir characterization: The Leading Edge, **18**, 353–360.

Stark, T. J., 2005, Generation of a 3D seismic "wheeler diagram" from a high resolution age volume: Expanded Abstracts 75^{th} SEG International Convention, **9**, 782–785.

Wolak, J., N. Hemstra, J. Ochoa, and M. Pelissier, 2013, Reconstruction of depocenter evolution through time using relative stratigraphic thickness: The Leading Edge, **32**, 172–177.

Zeng, H., S. C. Henry, and J. P. Riola, 1998, Stratal slicing, part ii: Real 3-D seismic data: Geophysics, **63**, no. 2, 514–522.